

## Band-gap shifts in heavily $p$ -type doped semiconductors of the zinc-blende and diamond type

Bo E. Sernelius\*

*Solid State Division, Oak Ridge National Laboratory, Oak Ridge, Tennessee 37831  
and Department of Physics, University of Tennessee, Knoxville, Tennessee 37916*

(Received 26 March 1986)

We present derivations of the band-gap shifts in, and photoluminescence spectra from, heavily doped  $p$ -type semiconductors of zinc-blende and diamond type. The calculated final-state lifetimes are taken into account in the derivation of the luminescence peaks. They stem from the imaginary parts of the self-energy shifts due to electron-electron and electron-dopant-ion scattering. These are derived within the same formalism as the real parts causing the band shifts. Our results are compared in detail to those from photoluminescence experiments on  $p$ -type GaAs. The lifetime broadening is found to explain fully the low-energy tailing of the luminescence peaks. No assumption of band tailing is needed.

### I. INTRODUCTION

The effect of heavy doping on the electronic states in semiconductors is both an interesting and important problem which has attracted an increasing interest both experimentally and theoretically. Experimentally it is a well-known fact that the bands are shifted in energy due to the presence of the ionized dopant ions and released charge carriers. We refer to Refs. 1 and 2 for an extensive list of references to earlier experimental and theoretical works and to Refs. 3–9 for the up-to-date theory.

The bands are shifted in such a way that the band gap decreases. However, the estimated band-gap narrowing varies among the different types of experiments. The band shifts are, in general, not rigid, i.e., different states are shifted different amounts. This causes a deformation of the density of states, for the conduction and valence bands. The amount of deviation from rigid band shifts varies from semiconductor to semiconductor and even within the same semiconductor it depends on the type of doping,  $n$  or  $p$  type. It also varies with doping level. This deviation from rigid band shifts means that the band-gap narrowing deduced from absorption and luminescence experiments might differ, as these experiments involve transitions between different sets of states. Thus, one has to specify what band-gap narrowing one is referring to.

Furthermore, it is very difficult to extract the "exact" band-gap shifts because of the lifetime-broadening effects. In the absorption measurements this shows up as a gradual, and not abrupt, absorption threshold and in the luminescence experiments the peaks are broadened, especially at the low-energy side.

Besides the band-gap narrowing an interesting question is whether there are any band-tailing effects. With band tailing one means the existence of a tail of localized states below the conduction-band edge and/or above the valence-band edge. These tails are expected to be caused by the disordered distribution of dopant ions. If they do exist they could easily be detected in the luminescence experiments were it not for the lifetime broadening, causing similar experimental effects. Some very nice experiments

in this context are the piezo experiments<sup>10,11</sup> on  $n$ -type many-valley semiconductors. As a mechanical stress is applied in a suitable symmetry direction electrons are transferred between the conduction-band valleys. The optical and transport properties of the sample are changed due to the resulting symmetry change. At a high stress point the electron transfer saturates as some of the valleys are completely emptied. The change in the properties close to the saturation point gives information about the density of states near the conduction-band edges. The experimental results pointed to strong band-tailing effects, but in Ref. 9 the same behavior was reproduced theoretically in the complete absence of band tailing. In Ref. 9 it was found that the electron transfer as a function of applied stress is modified by the energy shifts of the conduction-band states due to electron-electron and electron-donor-ion interactions. This modification was found to be such that the experimental behavior was reproduced. What is especially interesting is that the electron transfer is not influenced by any finite lifetimes.<sup>9</sup> The theoretical results were later supported by experiments on the extrinsic plasmon energies as functions of applied stress.<sup>12</sup>

The best way to circumvent the problems with the lifetime-broadening effects in the absorption and luminescence experiments is to theoretically determine the self-energy shifts for all states involved and calculate the theoretical spectra, including the effects from the calculated lifetime broadening. From the comparison between the experimental and theoretical results one can deduce an estimate of the "real" experimental band-gap narrowing. With "real" we mean the result one would obtain if the lifetime-broadening effects were absent. In contrast we let the "apparent" band gap denote the experimental band gap obtained by extrapolating the linear part of the low-energy side of the spectrum to zero intensity. We perform such comparisons between theoretical and experimental spectra for  $p$ -type GaAs in Sec. III. But first, in Sec. II we extend the theoretical model from Refs. 3 and 4 to  $p$ -type semiconductors of zinc-blende type, e.g., GaAs. These results are also valid for  $p$ -type semiconductors of

diamond type, like Si and Ge. This model worked well for *n*-type Si (Ref. 13) and GaAs (Ref. 8). The theory is much more involved for the *p*-type case because of the complicated valence bands. We present a somewhat simplified approach to get feasible results for *p*-type semiconductors. Finally, in Sec. IV, we make a summary and draw conclusions.

## II. DERIVATION OF SELF-ENERGY SHIFTS

In this section we will give a detailed derivation of the different self-energies, in a heavily doped semiconductor, due to the presence of the dopant. We use plane waves as basis states and rely on the effective-mass approximation. We assume that the doping level is so high that all dopant charge carriers have been released. These are holes in a *p*-type semiconductor and occupy the states at the top of the valence band. In calculating the self-energies we start from the total energy of this system of holes and dopant ions. Experiments estimating the band-gap change from doping always involve both states in the valence band and in the conduction band. In order to obtain as well the self-energy shifts for the conduction-band states we allow a few electrons to be present in the calculation of the total energy. We refer to these electrons as the few electrons in what follows. The total energy,  $E$ , can be divided into three contributions. The kinetic energy,  $E_{\text{kin}}$ , would be the only contribution if all interactions among the electrons, holes, and acceptor ions were neglected. The exchange and correlation energy,  $E_{\text{xc}}$ , could be divided into the exchange energy for the holes, the exchange energy for the electrons, and the correlation energy for the electron-hole system. We have no reason for making this separation here. Instead we treat this energy as one entity. The third, and last, contribution,  $E_{\text{eha}}$ , is due to the interaction between the particles and acceptor ions. Thus, we have made the following separation of the total energy:

$$E = E_{\text{kin}} + E_{\text{xc}} + E_{\text{eha}} . \quad (2.1)$$

The valence bands in GaAs are warped and coupled. This is treated in the same way as in Refs. 14 and 15. The bands are replaced by a heavy-hole band and a light-hole band whose dispersions are obtained by spherically averaging the real dispersions. The coupling between the bands is retained and the matrix elements for inter-valence-band and intra-valence-band processes are angle dependent. We will return to this, in more detail, later. With these approximations the kinetic energy is given by

$$E_{\text{kin}} = \sum_{\mathbf{k}, \sigma} e_{\mathbf{k}n}^j , \quad (2.2)$$

$j = e, hh, lh$

where  $e$ ,  $n$ ,  $\mathbf{k}$ , and  $\sigma$  denote kinetic energy, occupation number, wave vector, and spin, respectively. The index  $j$  runs over electrons, heavy holes, and light holes denoted by  $e$ ,  $hh$ , and  $lh$ , respectively. For the valence bands spin is not a good quantum number, however, but the four valence bands are still pairwise degenerate. We can use the same index  $\sigma$ , to run over the two degenerate bands.

The exchange and correlation energy can be expressed as

$$E_{\text{xc}} = - \int_0^1 \frac{d\lambda}{\lambda} \left[ \sum'_{\mathbf{q}} \left[ \int_0^\infty d\omega \frac{\hbar}{2\pi i} [\epsilon_\lambda^{-1}(\mathbf{q}, \omega) - 1] + \lambda \frac{Nv(\mathbf{q})}{2\kappa\Omega} \right] \right] , \quad (2.3)$$

where the first integral is over the coupling constant  $\lambda$ .  $\Omega$  denotes the volume of the system and  $v(\mathbf{q})$  is the Fourier-transformed Coulomb potential. The function  $\epsilon(\mathbf{q}, \omega)$  is the dielectric function for the combined system of holes and few electrons we consider. The prime over the  $\sum$  denotes, here and in what follows, that  $\mathbf{q}=0$  is omitted in the summation. All potentials are divided here by the background-screening constant,  $\kappa$ . We return to this point later. The second term comes from omitting the interaction of each particle with itself. Expressed in another way it is  $N$ , the number of particles, times the infinite energy contained in the electric field from a unit point charge. We rewrite this term to get a faster converging integral but also to take the opportunity to make the physics more transparent. We can rewrite Eq. (2.3) as

$$E_{\text{xc}} = - \int_0^1 d\lambda \frac{1}{\lambda} \sum'_{\mathbf{q}} \int_0^\infty d\omega \frac{\hbar}{2\pi i} \{ [\epsilon_\lambda^{-1}(\mathbf{q}, \omega) - 1] - [\epsilon_{0,\lambda}^{-1}(\mathbf{q}, \omega) - 1] \} , \quad (2.4)$$

where  $\epsilon_0(\mathbf{q}, \omega)$  is the dielectric function one would have for the system if the particles were occupying the same states as now, but were noninteracting and were not obeying the Pauli principle. With the last statement we mean that they are allowed to scatter into states already occupied. The indices  $\lambda$  on the dielectric functions indicate the functions for the particular coupling constant. We perform the calculation within the random-phase approximation (RPA) and are hence using the RPA dielectric function for  $\epsilon(\mathbf{q}, \omega)$ . If one wants to go beyond the pure RPA, i.e., include local field corrections, one should use the electron-test-particle dielectric function. If one is interested in the exchange energy one should use the Hartree-Fock dielectric function. This one is similar to  $\epsilon_0$  but in its derivation the particles are no longer allowed to scatter into already occupied states. Performing the integration over coupling constant, one obtains

$$E_{\text{xc}} = - \sum'_{\mathbf{q}} \int_0^\infty d\omega \frac{\hbar}{2\pi i} \{ -\ln\epsilon(\mathbf{q}, \omega) - [\epsilon_0^{-1}(\mathbf{q}, \omega) - 1] \} , \quad (2.5)$$

where we have used the fact that the second term of the integrand in Eq. (2.4) is proportional to  $\lambda$ .

Now, let us return to the fact that we have divided all potentials by  $\kappa$ , i.e., we have treated the system as if embedded in a dielectric medium, a medium unaffected by the presence of the system.

Now, let us prove that this is the correct approach and that we do not lose any contributions. What we are interested in is the change in the energy of the entire system due to the presence of the dopants. The origin of  $\kappa$  is the

polarizable valence electrons and to a lesser extent the polarizable core electrons.  $\kappa$  is not a constant but a function of the wave vector and frequency. However, it varies on the scale of a reciprocal lattice vector and on the scale of the band gap.

Let us now include all electrons in our system. The dielectric function of Eq. (2.3) was given by

$$\epsilon_\lambda = 1 + \lambda\alpha/\kappa, \quad (2.6)$$

where the function  $\alpha$  is the polarizability of the acceptor holes and few electrons, mentioned above. The dielectric function for the whole system can be written as

$$\epsilon'_\lambda = 1 + \lambda\beta + \lambda\alpha, \quad (2.7)$$

where  $\kappa$  has been expressed as

$$\kappa = 1 + \beta. \quad (2.8)$$

We have included a coupling constant in front of  $\beta$  as all electrons are treated on the same footing. Now we have to agree on a reference system. We are interested here in the change in energy for the electron states due to the presence of the acceptor holes. The energy of the reference system equals the sum of the  $N$  energy contributions obtained when particles are added to the system one at a time. When performing this summation one has to be careful not to multiple count the contributions from the interaction energies in the pure, undoped system. To avoid this multiple counting we subtract these energy contributions from each term in Eq. (2.9) below. An alternative way to obtain the energy of the reference system is, as in Eq. (2.4), to add all particles but assume that they are completely unaware of the presence of each other. Let  $\alpha'_{\mathbf{k},\sigma}$  denote the polarizability from a particle in the state specified by the indices  $\mathbf{k}$ ,  $\sigma$ , and  $j$ . Equation (2.4) is now replaced by

$$E_{xc} = - \int_0^1 d\lambda \frac{1}{\lambda} \sum'_q \int_0^\infty d\omega \frac{\hbar}{2\pi i} \left\{ \left[ \frac{1}{1 + \lambda\alpha + \lambda\beta} - 1 \right] - \left[ \frac{1}{1 + \lambda\beta} - 1 \right] - \sum_{\mathbf{k},\sigma,j} \left[ \left[ \frac{1}{1 + \lambda\alpha'_{\mathbf{k},\sigma} + \lambda\beta} - 1 \right] - \left[ \frac{1}{1 + \lambda\beta} - 1 \right] \right] \right\}. \quad (2.9)$$

Integration over coupling constant yields

$$\begin{aligned} E_{xc} &= - \sum'_q \int_0^\infty d\omega \frac{\hbar}{2\pi i} \left[ -\ln \left[ \frac{1 + \alpha + \beta}{1 + \beta} \right] + \sum_{\mathbf{k},\sigma,j} \ln \left[ \frac{1 + \alpha'_{\mathbf{k},\sigma} + \beta}{1 + \beta} \right] \right] \\ &= - \sum'_q \int_0^\infty d\omega \frac{\hbar}{2\pi i} \left[ -\ln[1 + \alpha/(1 + \beta)] + \sum_{\mathbf{k},\sigma,j} \ln[1 + \alpha'_{\mathbf{k},\sigma}/(1 + \beta)] \right] \\ &= - \sum'_q \int_0^\infty d\omega \frac{\hbar}{2\pi i} \left[ -\ln\epsilon(\mathbf{q},\omega) + \sum_{\mathbf{k},\sigma,j} \frac{\alpha'_{\mathbf{k},\sigma}}{\kappa} \right], \end{aligned} \quad (2.10)$$

which is identical to Eq. (2.5). In the last step we made use of the fact that  $\alpha'_{\mathbf{k},\sigma}$  is of the order  $1/N$ . The function  $\kappa$  depends on wave vector and frequency but the integrand gives important contributions only for wave numbers and frequencies less or of the order of the  $k_F$  and  $E_F$ , respectively. Here  $k_F$  and  $E_F$  denote the Fermi wave number and Fermi energy, respectively, for the acceptor holes. This means that  $\kappa$  can be replaced by its zero wave number, zero frequency value in most cases. At the highest doping levels, however, the wave-number dependence starts to have an effect on the results. The frequency dependence can always be neglected. The situation is quite different in polar semiconductors. In a polar semiconductor the coupling to optical phonons gives rise to frequency variations in  $\kappa$  for low frequencies. Equation (2.10) is valid also in that case. Here we have taken into account the effects of correlation among all electrons in the system. For a polar semiconductor one also includes

the correlation with the atoms. GaAs has a very weak polar coupling and it can be neglected. We have neglected one more thing in our derivation. Due to the presence of the acceptor holes the function  $\beta$  is modified. One part of  $\beta$  is due to virtual transitions from the top of the valence band across the band gap. Now a small fraction of these valence-band states are unoccupied and the corresponding contribution to  $\beta$  should be missing. The effect of this is very difficult to calculate. We believe it to be small and hence neglect it.

The interaction with the acceptor ions gives rise to an energy contribution which to second order in the impurity potential is given by<sup>16,17</sup>

$$E_{eha} = \frac{n}{2} \sum'_q \frac{|\omega_0(\mathbf{q})|^2}{\kappa\nu(\mathbf{q})} \alpha_s(\mathbf{q}) [\epsilon^{-1}(\mathbf{q},0) - 1], \quad (2.11)$$

where  $\omega_0$  and  $\alpha_s$  are the Fourier transforms of one impur-

ity potential and the structure factor for the ions, respectively. We will approximate here the impurity potentials with pure Coulomb potentials and assume a random distribution of ions. This reduces Eq. (2.11) to

$$E_{eha} = \frac{n}{2} \sum_{\mathbf{q}}' \frac{v(\mathbf{q})}{\kappa} [\epsilon^{-1}(\mathbf{q}, 0) - 1], \quad (2.12)$$

where  $n$  is the density of ions.

Here also we have divided all potentials by  $\kappa$ . If we do not do this and extend our system, as in the alternative derivation above, to include all electrons in the system, the only difference is that the 1 in Eq. (2.12) is replaced by  $\kappa$ . This change does not affect the energy of the states we are interested in. It is important if, e.g., one wants to estimate the change in binding of the crystal due to the presence of the acceptor ions. In that case the energy will include a term

$$E_{\text{bind}} = \frac{n}{2} \sum_{\mathbf{q}}' v(\mathbf{q}) [\kappa^{-1}(\mathbf{q}, 0) - 1], \quad (2.13)$$

representing the gain in energy when the core and valence electrons adjust themselves to the ion potentials.

Our basic equations are (2.1), (2.2), (2.5) [or (2.10)], and (2.12). These represent total energies and not energies per particle. From these energies we obtain the quasiparticle energy,  $E_p$ , for a particle in state  $p$  according to the following definition

$$E_p = \frac{\delta E}{\delta n_p} = e_p + \Sigma_p, \quad (2.14)$$

where  $e_p$  and  $\Sigma_p$  are the kinetic energy and self-energy, respectively, for a particle in state  $p$ . Equation (2.14) means that the energy of a particle in state  $p$  is defined as the change in the total energy of the system when a particle is added to state  $p$ , if this state is unoccupied. The energy of a particle in state  $p$  is minus the change in total energy when a particle is removed from state  $p$  if it is originally occupied. The self-energy,  $\Sigma$ , is due to the interaction and comes from Eqs. (2.5) and (2.12). Thus it can be separated into two parts, one from the electron-electron and one from electron-ion interactions. It con-

tains a real and an imaginary part. The real part gives the energy shift of the state due to the interactions. The imaginary part gives the particle lifetime.

Let us start deriving the self-energy for states in the conduction band. In calculating  $\Sigma_p^{c,e}$ , the self-energy for a state  $p$  in the conduction band due to electron-electron interaction, we need the expression for the second term of the integrand in Eq. (2.5)

$$[\epsilon_0^{-1}(\mathbf{q}, \omega) - 1] = - \sum_{\mathbf{k}, \sigma, j} \frac{\alpha_{\mathbf{k}, \sigma}^j}{\kappa}. \quad (2.15)$$

We defer the contributions from the valence band until they are needed. The contribution from the few electrons is given by

$$\sum_{\mathbf{k}, \sigma} \frac{\alpha_{\mathbf{k}, \sigma}^e}{\kappa} = - \frac{v(\mathbf{q})}{\kappa \hbar \Omega} \sum_{\mathbf{k}, \sigma} n_{\mathbf{k}, \sigma}^e \left[ \frac{1}{\omega + \omega(\mathbf{k}, \mathbf{q}) - i\eta} - \frac{1}{\omega - \omega(\mathbf{k}, \mathbf{q}) + i\eta} \right], \quad (2.16)$$

where

$$\omega(\mathbf{k}, \mathbf{q}) = (e_{\mathbf{k}+\mathbf{q}}^e - e_{\mathbf{k}}^e) / \hbar. \quad (2.17)$$

Here we see clearly how the occupation numbers enter the expression. In the first term of Eq. (2.5) the occupation numbers for the electrons enter the part of the polarizability coming from the few conduction-band electrons. We need the derivative of the polarizability with respect to an occupation number, which is given by

$$\frac{\delta \alpha^e(\mathbf{q}, \omega)}{\delta n_{\mathbf{p}, \sigma}^e} = - \frac{v(\mathbf{q})}{\kappa \hbar \Omega} [G_{0, \sigma}^e(\mathbf{p} + \mathbf{q}, e_p^e / \hbar + \omega) + G_{0, \sigma}^e(\mathbf{p} - \mathbf{q}, e_p^e / \hbar - \omega)], \quad (2.18)$$

where the index 0 on the Green's function,  $G$ , denotes the noninteracting function.

The self-energy for an electron in the conduction band due to the electron-electron interaction can now be found to be

$$\Sigma_p^{c,e} = - \frac{1}{\Omega} \sum_{\mathbf{q}}' \frac{v(\mathbf{q})}{\kappa} \left\{ \int_{-\infty}^{\infty} d\omega \frac{1}{2\pi i} \left[ G_{0, \sigma}^e(\mathbf{p} + \mathbf{q}, e_p^e / \hbar + \omega) / \epsilon(\mathbf{q}, \omega) + \frac{1}{2} \left[ \frac{1}{\omega + \omega(\mathbf{p}, \mathbf{q}) - i\eta} - \frac{1}{\omega - \omega(\mathbf{p}, \mathbf{q}) + i\eta} \right] \right] \right\}, \quad (2.19)$$

where we have made use of the fact that the time-ordered dielectric function is even in  $\omega$  and have extended the integration region to include negative frequencies. As no magnetic field is present, the self-energy is independent of the particle spin, so we have dropped the index  $\sigma$ . If we start from Eq. (2.3), instead of Eq. (2.5), we obtain

$$\Sigma_p^{c,e} = - \frac{1}{\Omega} \sum_{\mathbf{q}}' \frac{v(\mathbf{q})}{\kappa} \left[ \int_{-\infty}^{\infty} d\omega \frac{1}{2\pi i} [G_{0, \sigma}^e(\mathbf{p} + \mathbf{q}, e_p^e / \hbar + \omega) / \epsilon(\mathbf{q}, \omega)] + \frac{1}{2} \right]. \quad (2.20)$$

Performing the derivative with respect to occupation number on Eq. (2.12), we obtain the following result for the self-energy due to the interaction with the ions:

$$\Sigma_p^{c,i} = \frac{n}{\hbar\Omega} \sum_q' \left[ \frac{v(\mathbf{q})}{\kappa\epsilon(\mathbf{q},0)} \right]^2 G_0^e(\mathbf{p}+\mathbf{q}, e_p^e/\hbar). \quad (2.21)$$

Before we perform the analogous derivations for the states in the valence bands we have to describe the polarizability from the acceptor holes in more detail. The energy dispersions of the valence bands in zinc-blende and diamond-type semiconductors are given by

$$E(\mathbf{k}) = Ak^2 \pm [B^2k^4 + C^2(k_x^2k_y^2 + k_x^2k_z^2 + k_y^2k_z^2)]^{1/2}, \quad (2.22)$$

i.e., the bands are parabolic in all directions but cubically warped. We neglect this warping as is usually done.<sup>14,15,18-20</sup> In doing this we get four pairwise degenerate hole bands,<sup>14,15,20</sup> two heavy-hole bands, and two light-hole bands. They are all degenerate for  $\mathbf{k}=0$ . The matrix elements between states in like bands are different from those between states in unlike bands.  $v(\mathbf{q})$  for processes between  $\mathbf{k}$  and  $\mathbf{k}+\mathbf{q}$  is replaced here by  $V_{11}$  for like bands and by  $V_{12}$  for unlike bands, where

$$V_{11} = v(\mathbf{q})(1 + 3 \cos^2[\mathbf{k}, \mathbf{k}+\mathbf{q}])/8, \quad (2.23)$$

and

$$V_{12} = v(\mathbf{q})3 \sin^2[\mathbf{k}, \mathbf{k}+\mathbf{q}]/8. \quad (2.24)$$

The polarizability can with these approximations be expressed as

$$\begin{aligned} \alpha(\mathbf{q}, \omega) = & \frac{1}{\kappa\hbar\Omega} \sum_{j,l=1}^2 \sum_{\mathbf{k}} \int_{-\infty}^{\infty} d\varepsilon \frac{1}{2\pi i} \{ [G_{0,j}^{hh}(\mathbf{k}, \varepsilon)G_{0,l}^{hh}(\mathbf{k}+\mathbf{q}, \varepsilon+\omega) + G_{0,j}^{lh}(\mathbf{k}, \varepsilon)G_{0,l}^{lh}(\mathbf{k}+\mathbf{q}, \varepsilon+\omega)] V_{11}(\mathbf{k}, \mathbf{k}+\mathbf{q}) \\ & + [G_{0,j}^{hh}(\mathbf{k}, \varepsilon)G_{0,l}^{lh}(\mathbf{k}+\mathbf{q}, \varepsilon+\omega) \\ & + G_{0,j}^{lh}(\mathbf{k}, \varepsilon)G_{0,l}^{hh}(\mathbf{k}+\mathbf{q}, \varepsilon+\omega)] V_{12}(\mathbf{k}, \mathbf{k}+\mathbf{q}) \}. \end{aligned} \quad (2.25)$$

The contribution from the holes to Eq. (2.15) is

$$[\epsilon_0^{-1}(\mathbf{q}, \omega) - 1]_{\text{holes}} = - \sum_{\substack{\mathbf{k}, \sigma \\ j=hh, lh}} \frac{\alpha_{\mathbf{k}, \sigma}^j}{\kappa}, \quad (2.26)$$

where

$$\begin{aligned} \alpha_{\mathbf{k}, \sigma}^j = & - \frac{2n_{\mathbf{k}, \sigma}^j}{\hbar\Omega} \left[ \left[ \frac{1}{\omega + \omega^{j,j}(\mathbf{k}, \mathbf{q}) - i\eta} - \frac{1}{\omega - \omega^{j,j}(\mathbf{k}, \mathbf{q}) + i\eta} \right] V_{11} \right. \\ & \left. + \left[ \frac{1}{\omega + \omega^{j,l(\neq j)}(\mathbf{k}, \mathbf{q}) - i\eta} - \frac{1}{\omega - \omega^{j,l(\neq j)}(\mathbf{k}, \mathbf{q}) + i\eta} \right] V_{12} \right] \end{aligned} \quad (2.27)$$

and

$$\omega^{j,l}(\mathbf{k}, \mathbf{q}) = (e_{\mathbf{k}+\mathbf{q}}^l - e_{\mathbf{k}}^j)/\hbar. \quad (2.28)$$

Taking the derivative with respect to occupation number of Eq. (2.25), we obtain

$$\begin{aligned} \frac{\delta\alpha(\mathbf{q}, \omega)}{\delta n_p^j} = & \frac{2}{\kappa\hbar\Omega} \{ [G_0^j(\mathbf{p}+\mathbf{q}, e_p^j/\hbar + \omega) + G_0^j(\mathbf{p}-\mathbf{q}, e_p^j/\hbar - \omega)] V_{11}(\mathbf{p}, \mathbf{p}+\mathbf{q}) \\ & + [G_0^{l(\neq j)}(\mathbf{p}+\mathbf{q}, e_p^l/\hbar + \omega) + G_0^{l(\neq j)}(\mathbf{p}-\mathbf{q}, e_p^l/\hbar - \omega)] V_{12}(\mathbf{p}, \mathbf{p}+\mathbf{q}) \}, \end{aligned} \quad (2.29)$$

where we have dropped the index  $\sigma$ . We can do this as the two like bands are completely equivalent for the present calculation.

Using these results we get the following contribution to the self-energy, for a hole state, from the electron-electron interaction:

$$\begin{aligned} \Sigma_p^{j,e} = & - \frac{2}{\kappa\Omega} \sum_q' \int_{-\infty}^{\infty} d\omega \frac{1}{2\pi i} \left\{ \left[ G_0^j(\mathbf{p}+\mathbf{q}, e_p^j/\hbar + \omega)/\epsilon(\mathbf{q}, \omega) \right. \right. \\ & \left. \left. + \frac{1}{2} \left[ \frac{1}{\omega + \omega^{j,j}(\mathbf{p}, \mathbf{q}) - i\eta} - \frac{1}{\omega - \omega^{j,j}(\mathbf{p}, \mathbf{q}) + i\eta} \right] \right] V_{11}(\mathbf{p}, \mathbf{p}+\mathbf{q}) \right. \\ & \left. + \left[ G_0^{l(\neq j)}(\mathbf{p}+\mathbf{q}, e_p^l/\hbar + \omega)/\epsilon(\mathbf{q}, \omega) \right. \right. \\ & \left. \left. + \frac{1}{2} \left[ \frac{1}{\omega + \omega^{j,l(\neq j)}(\mathbf{p}, \mathbf{q}) - i\eta} - \frac{1}{\omega - \omega^{j,l(\neq j)}(\mathbf{p}, \mathbf{q}) + i\eta} \right] \right] V_{12}(\mathbf{p}, \mathbf{p}+\mathbf{q}) \right\}. \end{aligned} \quad (2.30)$$

In treating the self-interaction as in Eq. (2.3) we get the following result, analogous to that in Eq. (2.20)

$$\Sigma_p^{j,e} = -\frac{1}{\kappa\Omega} \sum_q' \left[ 2 \int_{-\infty}^{\infty} d\omega \frac{1}{2\pi i} [V_{11}(\mathbf{p}, \mathbf{p}+\mathbf{q}) G_0^j(\mathbf{p}+\mathbf{q}, e_p^j/\hbar+\omega) + V_{12}(\mathbf{p}, \mathbf{p}+\mathbf{q}) G_0^{l(\neq j)}(\mathbf{p}+\mathbf{q}, e_p^l/\hbar+\omega)] / \epsilon(\mathbf{q}, \omega) + \frac{1}{2} \right]. \quad (2.31)$$

The contribution from interactions with the impurities is

$$\Sigma_p^{j,i} = \frac{2n}{\hbar\Omega} \sum_q' \left[ \frac{v(\mathbf{q})}{\kappa\epsilon(\mathbf{q}, 0)} \right]^2 \left[ \frac{V_{11}(\mathbf{p}, \mathbf{p}+\mathbf{q})}{v(\mathbf{q})} G_0^j(\mathbf{p}+\mathbf{q}, e_p^j/\hbar+\omega) + \frac{V_{12}(\mathbf{p}, \mathbf{p}+\mathbf{q})}{v(\mathbf{q})} G_0^{l(\neq j)}(\mathbf{p}+\mathbf{q}, e_p^l/\hbar+\omega) \right]. \quad (2.32)$$

The results we need for the calculation are contained in Eqs. (2.19), (2.21), (2.30), and (2.32). The dielectric function entering these equations is given by 1 plus the polarizability from Eq. (2.25). Note that the contribution from the few electrons is no longer present. It was needed in obtaining the derivative with respect to the conduction-band occupation number. The presence of the few electrons was then crucial but has now negligible effect on the screening.

The dielectric function is too complicated to be obtained in analytical form. To make the calculation feasible we approximate it by the result for completely decoupled valence bands, i.e., we replace  $V_{11}$  by  $v(q)/2$  and  $V_{12}$  by zero. We believe that the most important effects from the coupling are still retained and that this approximation will only have minor effects on the results. The contribution to the self-energy shifts from the exchange energy is not affected at all by this approximation.

The calculation of the contributions from the interaction with the ions is straightforward but the electron-electron part needs some comments. The integrations over  $\omega$  in Eqs. (2.19) and (2.30) are along the real  $\omega$  axis. We deform the integration path according to Fig. 2 in Ref. 4, and instead end up with an integration along the imaginary axis of the complex  $\omega$  plane. In addition we obtain residue contributions from the poles within the integration path. One usually denotes these different contributions as line and residue parts. The line parts are real and give no contribution to the particle lifetime. The residue contributions are complex. The separation between line and residue parts is, however, not unique. As an example of this we note that the self-interaction term in Eqs. (2.19) and (2.30) gives both a line and a residue contribution. In Eqs. (2.20) and (2.31), however, the same contribution does not belong to either.

We feel we should mention some particular points from the actual calculation. In the calculation of the residue parts one ends up with a numerical integration over a limited part of the  $\omega q$  plane. The limits are determined by the phase space available into which the particle in question may decay. In the calculation of the imaginary parts the integrand gives contributions only in the region of electron-hole pair excitations and on the plasmon line. These calculations are not trivial and have to be performed with care to avoid numerical problems. We will not go into this in detail. What we want to mention is a trick we used to avoid numerical problems in calculating

the real part. When the kinetic energy of an electron in the conduction band is larger than the plasmon energy for the valence-band holes, the integration region includes a part of the plasmon line. On the plasmon line the integral diverges. However, this divergency is integrable, but still causes numerical problems. We could circumvent these problems by using the following sum rule:

$$\int_0^{\infty} d\omega \operatorname{Re}[\epsilon^{-1}(\mathbf{q}, \omega) - 1] = 0. \quad (2.33)$$

Our frequency integral could be cast on the following form:

$$\operatorname{Re} \left[ \int_0^{\omega^{\max}(\mathbf{q})} d\omega [\epsilon^{-1}(\mathbf{q}, \omega) - 1] \right] = -\operatorname{Re} \left[ \int_{\omega^{\max}(\mathbf{q})}^{\infty} d\omega [\epsilon^{-1}(\mathbf{q}, \omega) - 1] \right], \quad (2.34)$$

and for every  $\mathbf{q}$  we were allowed to choose either of the expressions on the two sides of the equation. In that way we could avoid integrating over the plasmon line.

Another thing is worth mentioning. The light- and heavy-hole states with zero wave number are both shifted the same amount from the interactions. This is, however, not true for states with larger wave numbers. This causes a problem when dealing with *p*-doped semiconductors. When we start our calculation, before the interaction is turned on, the Fermi energy is the same in both hole bands. After the states have been shifted in energy, the states with Fermi wave vector no longer have the same energy in the heavy- and light-hole bands. This means that the holes will redistribute themselves. What we did was to redistribute the holes, perform the calculation, redistribute them again and so on until convergence. These were problems we had to encounter. The solution was more time consuming, but the results were only marginally influenced by this.

Before we show the results we need to introduce some more notation. Let  $E_g$  denote the unperturbed band gap. We introduce  $E_{g,1}$ ,  $E_{g,2}$ ,  $E_{g,3}$ , and  $E_{g,4}$ .  $E_{g,1}$  is the distance in energy from the bottom of the conduction band to the top of the valence band, and would equal  $E_g$  were it not for the interactions. With  $E_{g,2}$  and  $E_{g,3}$  we mean the difference in energy between states at  $k_{F_{lh}}$  in the conduction band and the heavy-hole band, and in the conduction band and light-hole band, respectively. Finally,  $E_{g,4}$  denotes the energy difference between states at  $k_{F_{hh}}$  in the conduction band and in the heavy-hole band.  $k_{F_{lh}}$  and

$k_{F_{hh}}$  represent the Fermi momentum in the light-hole and heavy-hole band, respectively. The band-gap shifts are defined as follows

$$\Delta E_{g,i} = E_{g,i} - E_g; \quad i = 1, 2, 3, 4. \quad (2.35)$$

We should further point out that we treat the particles in the valence bands as holes, i.e., the kinetic energy increases with wave number and the Green's functions in Eqs. (2.25)–(2.32) are hole Green's functions with hole-occupation numbers. With this convention all self-energies are negative and the similarity between the electrons in the conduction band and the holes in the valence band is more transparent. In order to compare our results to experiments at different temperatures we subtract the unperturbed band-gap values from the experimental energies. At 4.2, 20, 77, and 300 K we use the values 1.518, 1.521, 1.512, and 1.426 eV, respectively. Furthermore, we use for the electron mass, heavy-hole mass, and light-hole mass the values 0.0665, 0.45, and 0.082, respectively. For  $\kappa$  we use the value 13.0. All these data are from Ref. 21.

Figure 1 shows the different band-gap shifts as functions of the acceptor concentration,  $n$ . The circles represent the experimental luminescence-peak positions obtained at 77 K, in Ref. 22. The origin of the luminescence peaks is the recombination between a small quantity of thermalized electrons at the bottom of the conduction band and holes at the top of the valence bands. We make a more detailed comparison in the next section, but it is interesting to see the correlation between the peak positions and  $\Delta E_{g,1}$ , which is an estimate of the expected low-energy edge of the peaks. In Fig. 2 we have expanded the scales and added some experimental luminescence peaks. The curves  $P_1$  and  $P_3$  are from Ref. 22, and  $P_2$  is

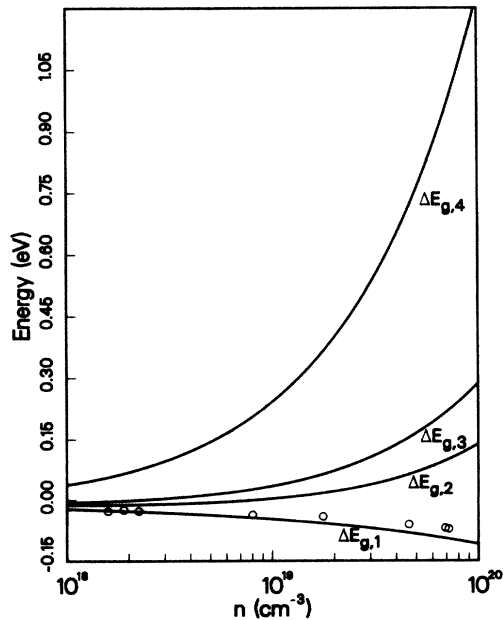


FIG. 1. The different band-gap shifts, defined in the text, as functions of the acceptor density,  $n$ . The circles represent the experimental luminescence-peak positions obtained in Ref. 22, at 77 K.

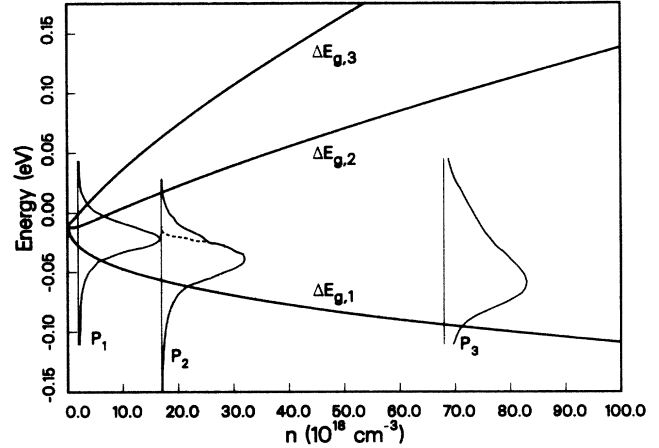


FIG. 2. The different band-gap shifts, defined in the text, as functions of the acceptor density,  $n$ . The luminescence peaks  $P_1$  and  $P_3$  are from Ref. 22 and  $P_2$  is from Ref. 23. They were all obtained at 77 K.

from Ref. 23, all obtained at 77 K. We find that it is difficult to define the low-energy threshold for the peaks. Figure 3 shows the different self-energy contributions to  $\Delta E_{g,1}$ . Both the light- and heavy-hole bands are shifted the same amount at  $\mathbf{k}=0$ . Hence we use  $\nu$ , as in the valence band, to indicate these shifts. We find in Figs. 1 and 3 that the shifts are much more modest for the doped  $p$ -type case than was found in the doped  $n$ -type case.<sup>8</sup>

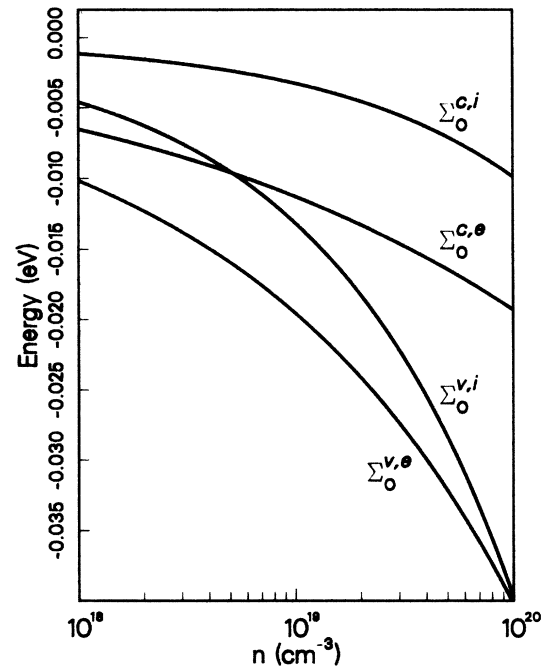


FIG. 3. The different self-energy contributions to  $\Delta E_{g,1}$ . The indices  $\nu$  and  $c$  indicate that the shifted states are in the valence and conduction band, respectively, while  $e$  and  $i$  distinguish between contributions from electron-electron and electron-ion interactions. Finally the index 0 specifies that the states in question have zero wave numbers.

The same was found experimentally in Ref. 22. This is because of the much more effective screening from the holes in the *p*-type case, due to their larger effective mass.

In the next section we calculate the theoretical luminescence peaks in order to get a more detailed comparison between theory and experiments.

### III. DERIVATION OF THE LUMINESCENCE SPECTRA

In this section we derive the theoretical photoluminescence peaks and compare these to the experimental ones. The results are based on the following assumptions. We assume that the electrons taking part in the recombination processes are completely thermalized. We do not know the number of electrons that are collected at the bottom of the conduction band. We use this number as an adjustable parameter when comparing the results to experiments. We further approximate the matrix elements for the pro-

cesses with a constant and assume that this constant is the same for both hole types.

The photoluminescence intensity can with these assumptions be expressed as

$$I_{\text{PL}}(h\nu) = \sum_{j=\text{lh, hh}} I_{\text{PL}}^j(h\nu), \quad (3.1)$$

where

$$I_{\text{PL}}^j(h\nu) = \int d\mathbf{k} \int d\mathbf{k}' f(e_{\mathbf{k}}^e + \text{Re}\Sigma_{\mathbf{k}}^e) f(e_{\mathbf{k}'}^h + \text{Re}\Sigma_{\mathbf{k}'}^h) \times A(\mathbf{k}, \mathbf{k}', h\nu), \quad (3.2)$$

in its most general form. The functions  $f$  are the Fermi-Dirac distribution functions for the two particle types taking part in the processes. The energy  $h\nu$  is the photon energy after subtraction of the value of the unperturbed band gap  $E_g$ . We have used the following expression for the function  $A$

$$A(\mathbf{k}, \mathbf{k}', h\nu) = -\delta(\mathbf{k} - \mathbf{k}') \frac{1}{\pi} \frac{\text{Im}(\Sigma_{\mathbf{k}}^e + \Sigma_{\mathbf{k}'}^h)}{\text{Im}^2(\Sigma_{\mathbf{k}}^e + \Sigma_{\mathbf{k}'}^h) + [e_{\mathbf{k}}^e + e_{\mathbf{k}'}^h + \text{Re}(\Sigma_{\mathbf{k}}^e + \Sigma_{\mathbf{k}'}^h) - h\nu]^2}. \quad (3.3)$$

We have assumed  $\mathbf{k}$  conservation. If one wants to calculate the result for nonvertical transitions, one omits the delta function. This is the proper choice for indirect-gap semiconductors like Si and Ge. That version should also be used if one wants to estimate the contribution from non- $\mathbf{k}$ -conserving processes due to the presence of the acceptor ions. It should be pointed out that the expression we use is not theoretically well founded. It should be regarded as an approximation or a model.

If the finite lifetimes are neglected the function  $A$  transforms into

$$A(\mathbf{k}, \mathbf{k}', h\nu) = \delta(\mathbf{k} - \mathbf{k}') \delta(h\nu - [e_{\mathbf{k}}^e + e_{\mathbf{k}'}^h + \text{Re}(\Sigma_{\mathbf{k}}^e + \Sigma_{\mathbf{k}'}^h)]). \quad (3.4)$$

Equation (3.2) with the non- $\mathbf{k}$ -conserving version of this function was used in Ref. 13 to study the photoluminescence in Si.

In Fig. 4 we show our result for the acceptor density  $6.8 \times 10^{19} \text{ cm}^{-3}$  at 77 K. The solid curve gives the full result, while the dashed and dotted curves represent the contributions from heavy and light holes, respectively. The experimental peak from Ref. 22 is shown by the dash-dotted curve. The corresponding comparison between theory and experiment for a sample with density  $4 \times 10^{19} \text{ cm}^{-3}$  and at the lower temperature 15 K is shown in Fig. 5. Here the experimental curve is from Ref. 24. In the comparison we have normalized the curves to the same peak value, varied the chemical potential in the conduction band, and rigidly shifted the theoretical peaks. In Figs. 4 and 5 these shifts were 15 and 11 meV, respectively. These shifts can be regarded as the deviation between theoretical and experimental band-gap shifts. The overall agreement between the experimental and theoretical peak shapes was found to be very good. The experimental

broadening on the low-energy side was reproduced by the lifetime broadening. One should note that the lifetime broadening was really calculated and was not used as an adjustable parameter. We compared our results to experimental peaks in a large density range and found this good agreement in all cases. The peak or shoulder on the high-

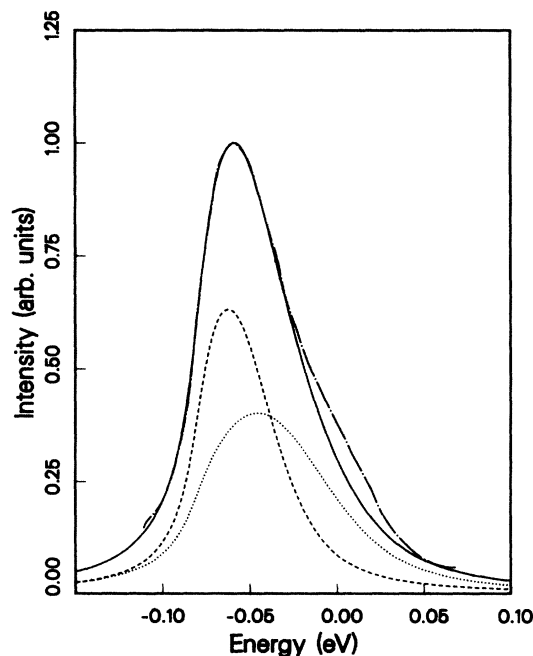


FIG. 4. Comparison between the theoretical, solid curve, and experimental, dash-dotted curve, photoluminescence peaks for a sample with acceptor concentration  $6.8 \times 10^{19} \text{ cm}^{-3}$  at 77 K. The experimental peak is from Ref. 22. The dashed and dotted curves show the contribution from recombination with heavy and light holes, respectively.



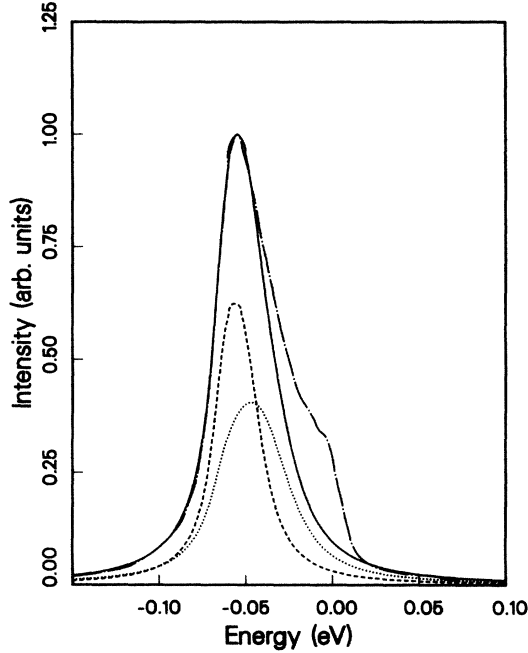


FIG. 5. The same as in Fig. 4 except now for a sample from Ref. 24 with density  $4 \times 10^{19} \text{ cm}^{-3}$  and obtained at 15 K.

energy side of the peaks seems to be common to all spectra from high-density samples. In many papers<sup>24–27</sup> this structure has been interpreted as coming from non- $\mathbf{k}$ -conserving processes due to the presence of the acceptor ions. In these papers the upper edge of this structure is referred to as  $E_0 + E_F$ , i.e., its energy position is expected to be at the value of  $\Delta E_{g,1}$  plus the Fermi energy. However if this were the case the upper edge would be at 0.07 and 0.04 eV in Figs. 4 and 5, respectively. Taking the finite width of the electron distribution in the conduction

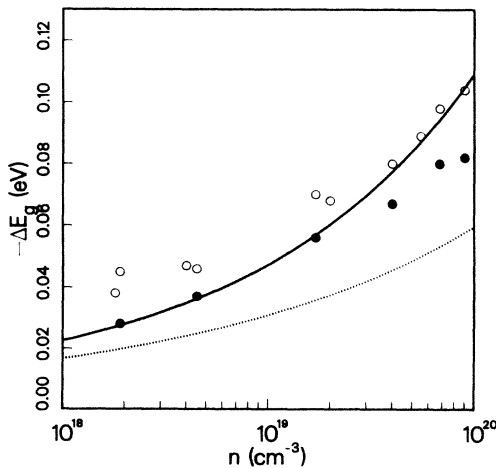


FIG. 6. “Real,” solid circles, and “apparent,” open circles, experimental band-gap narrowing, compared to the theoretical results, solid curve. The dotted curve is the result obtained neglecting the interaction with the acceptor ions. The experiments are from Refs. 22 and 24–26.

band into account the upper edge would move to even higher energies. From this we can conclude that the canonical explanation for this structure must be wrong.

We close this section by showing in Fig. 6 a plot of our result for the band-gap narrowing in comparison with experiments. The solid curve is the theoretical result. The open circles are experimental so-called “apparent” band-gap shifts, obtained from Refs. 22 and 24–26, by extrapolating the low-energy edges of the peaks to the background. The solid circles represent the “real” band gaps obtained from the comparison between the experimental and theoretical luminescence peaks. The dotted curve is the theoretical result if all interactions with the acceptor ions are neglected.

#### IV. SUMMARY AND CONCLUSIONS

We have presented a derivation of the energy shifts, due to doping, for the conduction- and valence-band states in doped  $p$ -type semiconductors of zinc-blende and diamond type. The complications caused by the coupling between the valence bands were considered in an approximate way. The results were compared to those from photoluminescence on doped  $p$ -type GaAs. Because of the finite lifetime for the final states the luminescence peaks are broadened. This makes the experimental extraction of the band shifts difficult. To get reliable estimates we calculated the expected photoluminescence peaks, taking the lifetime broadening into account. The lifetimes of the final states were obtained from the imaginary parts of the self-energy shifts. The self-energy shifts contain contributions from electron-electron and electron-dopant-ion interactions. The real parts cause the band shifts and the imaginary parts the finite lifetimes, giving rise to the peak broadening. The real and imaginary parts were calculated quite consistently. The peak shapes agreed to such an extent that a “real” band-gap narrowing could be obtained with the use of the experimental and theoretical peaks. We use “real” to denote the shifts which would be obtained in experiments where no lifetime effects are present. In contrast, the “apparent” band-gap narrowing denotes the narrowing obtained by extrapolating the low-energy side of the peaks to the background.

Two things, in particular, were noted in the comparison between the theoretical and experimental photoluminescence peaks. First of all, the tailing of the low-energy side of the peaks, often believed to be due to band tailing caused by fluctuations in the dopant concentration, was fully reproduced by the lifetime broadening. The second thing concerns the high-energy shoulder, which seems to be common to all high-density samples, and which in numerous papers is referred to as being due to non- $\mathbf{k}$ -conserving processes. We found that its position was so far off in energy that this explanation must be wrong. This peak seems to be located at an energy slightly lower than the energy of the band gap in the pure crystal. One possible, but rather speculative, explanation for this peak is the following. Assume there is a depletion region or an undoped region somewhere in the sample. In this region the size of the band gap is expected to be equal to that of the pure crystal. Electrons excited to the conduction band

just inside this region can recombine with holes from the "normal" part of the crystal, preferably with those close to the Fermi level, as those have wave functions extending furthest into the depletion region. The Fermi level will, for the highest doping levels, be just above the position of the valence-band edge, in the depletion region, and move upwards for lower doping levels. This is consistent with the experimental behavior.

The theoretical band-gap narrowing showed an almost perfect agreement with the "real" band-gap narrowing for densities up to  $\sim 2 \times 10^{19}$ . For higher densities the theory gave values that were too high. In spite of this it was clearly demonstrated that the electron-ion-interaction contribution, used in our approach, improved the agreement considerably over what would be obtained if it was neglected. The agreement also strengthens the belief that the distribution of ions is random and not of superlattice type as suggested in Ref. 28. A distribution of the acceptors on a superlattice would give a nearly negligible electron-ion contribution.<sup>7</sup> The agreement with experiments obtained here and in Ref. 8 indirectly favors the approach presented in Refs. 3, 4, and 7 for *n*-type Si over that described in Refs. 28 and 29. In the latter two references one assumed that the ions were distributed on a superlattice and found large intervalley and negligible intravalley contributions. The intervalley contributions were similar to the intravalley contributions in Ref. 4 and the agreement with experiments was good in both approaches. In GaAs there is only one conduction-band minimum, in contrast to the six equivalent band minima in Si, so here the intervalley contributions are undoubtedly absent.

We cannot give a conclusive explanation for the deviation between the theory and experiment at the high-density limit, but merely speculate. It could be due to our approximate treatment of the coupling between the valence bands. If the resulting screening from the dopant

holes is too weak the correlation energy and the energy from the interactions with the ions become too large. One would in that case expect to find a deviation like the one in Fig. 6. Another possibility is that the deviation is due to our using a pure Coulomb potential for the electron-ion interaction, and not a more realistic pseudopotential. The effects of this will increase with density. The deviation does not depend on the fact that the dopant positions are restricted to host-atom positions. This will also cause deviations from higher densities and the deviations will be in the right direction. These effects, however, are very small in the density range considered here. We have tested this by using a hard-sphere structure factor,<sup>30-32</sup> simulating the situation where no two Zn atoms can be closer to each other than the nearest distance between two Ga atoms. The effect was negligible.

Finally, we should also bear in mind that the "real" band gaps have several experimental uncertainties attached to them. These include the uncertainty in the energy measurement and in the experimental pure band-gap value. It also includes uncertainties due to the difficulties in estimating the carrier concentration, effects from possible self-compensation and impurity clustering. What we have done is to eliminate the error in the interpretation of the experiments and in the extraction of the band-gap shifts.

#### ACKNOWLEDGMENTS

Research support is acknowledged from the University of Tennessee, Oak Ridge National Laboratory, and the U.S. Department of Energy (through the Oak Ridge National Laboratory, operated by Martin Marietta Energy Systems, Inc.), under Contract No. DE-AC05-84OR21400. Support from the Swedish Natural Science Research Council is also acknowledged.

\*Permanent address: Department of Physics and Measurement Technology, University of Linköping, S-581 83 Linköping, Sweden.

<sup>1</sup>R. W. Keyes, *Comments Solid State Phys.* **7**, 149 (1977).

<sup>2</sup>R. A. Abram, G. J. Rees, and B. L. H. Wilson, *Adv. Phys.* **27**, 799 (1978).

<sup>3</sup>B. E. Sernelius and K.-F. Berggren, in *Recent Developments in Condensed Matter Physics*, edited by J. T. Devreese, L. F. Lemmens, V. E. Van Doren, and J. Van Royen (Plenum, New York, 1981), Vol. 3.

<sup>4</sup>K.-F. Berggren and B. E. Sernelius, *Phys. Rev. B* **24**, 1971 (1981).

<sup>5</sup>G. D. Mahan, *J. Appl. Phys.* **15**, 2634 (1980).

<sup>6</sup>I. Hamberg, C. G. Granqvist, K.-F. Berggren, B. E. Sernelius, and L. Engström, *Phys. Rev. B* **30**, 3240 (1984).

<sup>7</sup>K.-F. Berggren and B. E. Sernelius, *Phys. Rev. B* **29**, 5575 (1984).

<sup>8</sup>B. E. Sernelius, *Phys. Rev. B* **33**, 8582 (1986).

<sup>9</sup>B. E. Sernelius, *Phys. Rev. B* **27**, 6234 (1983).

<sup>10</sup>H. Fritzsche, *J. Phys. Chem. Solids* **6**, 69 (1958).

<sup>11</sup>A. Feldman, *Phys. Rev.* **150**, 758 (1966).

<sup>12</sup>F. Cerdeira, N. Mestres, and M. Cardona, *Phys. Rev. B* **29**, 3737 (1984).

<sup>13</sup>J. Wagner, *Phys. Rev. B* **32**, 1323 (1985).

<sup>14</sup>M. Combescot and P. Nozières, *Solid State Commun.* **10**, 301 (1972).

<sup>15</sup>M. Combescot and P. Nozières, *J. Phys. C* **5**, 2369 (1972).

<sup>16</sup>B. E. Sernelius, University of Linköping Report No. ISBN-91-7372-8, 1978 (unpublished).

<sup>17</sup>B. E. Sernelius and K.-F. Berggren, *Philos. Mag. B* **43**, 115 (1981).

<sup>18</sup>J. M. Luttinger and W. Kohn, *Phys. Rev.* **97**, 869 (1955).

<sup>19</sup>W. F. Brinkman and T. M. Rice, *Phys. Rev. B* **7**, 1508 (1973).

<sup>20</sup>G. Beni and T. M. Rice, *Phys. Rev. B* **18**, 768 (1978).

<sup>21</sup>*Numerical Data and Functional Relationships in Science and Technology*, Vol. III/17a of *Landolt-Börnstein*, edited by O. Madelung (Springer, Heidelberg, 1982).

<sup>22</sup>M. I. Nathan, G. Burns, S. E. Blum, and J. C. Marinace, *Phys. Rev.* **132**, 1482 (1963).

<sup>23</sup>D. E. Hill, *Phys. Rev.* **133**, A866 (1964).

<sup>24</sup>D. Olego and M. Cardona, *Phys. Rev. B* **22**, 886 (1980).

<sup>25</sup>A. N. Titkov, E. I. Chaikina, É. M. Komova, and N. G. Ermakova, *Fiz. Tekh. Poluprovodn.* **15**, 345 (1981) [*Sov. Phys. Semicond.* **15**, 198 (1981)].

<sup>26</sup>R. C. Miller, D. A. Kleinman, W. A. Nordland, Jr., and R. A. Logan, *Phys. Rev. B* **23**, 4399 (1981).

<sup>27</sup>A. Twardowski and C. Hermann, *Phys. Rev. B* **32**, 8253 (1985).

- <sup>28</sup>S. T. Pantelides, A. Selloni, and R. Car, *Solid State Electron.* **28**, 17 (1985).
- <sup>29</sup>A. Selloni and S. T. Pantelides, *Phys. Rev. Lett.* **49**, 586 (1983).

- <sup>30</sup>J. K. Percus and G. J. Yevick, *Phys. Rev.* **110**, 1 (1958).
- <sup>31</sup>J. L. Lebowitz, *Phys. Rev.* **133**, A895 (1964).
- <sup>32</sup>N. W. Ashcroft and D. C. Langreth, *Phys. Rev.* **156**, 685 (1967).